Journal of Engineering and Technological Advances (JETA)
https://jeta.segi.edu.my/index.php/segi
2024 Vol. 10 No. 2

METALLURGICAL FAILURE ANALYSIS OF A TRICYCLE FRONT WHEEL AXLE

Muazu, A.*, Yusuf, T., Jamilu, S., Abusufyan, S. K., Elijah, U. E., Joshua, I.
Department of Mechanical Engineering, Bayero University, Kano, Nigeria.
* Corresponding Author: amuazu.mec@buk.edu.ng

Received: 31 July 2024; Accepted: 09 September 2024; Published: 31 December 2024
doi: 10.35934/segi.v10i2.111

Highlights:

- Tricycle front wheel axle.
- Microstructure of core and surface of axle.
- Hardness of core and surface of axle.

Abstract: Due to the rampant failure of the tricycle front wheel axle in Nigeria, the failure analysis of a tricycle front wheel axle was conducted in this work. The failed front wheel axle of the tricycle part was obtained. Chemical composition, microhardness and microstructures through metallography and SEM were performed. The results show the carbon content of the failed axle wheel (0.354 wt% C) is below standard. The hardness results showed that the failed material probably had not undergone proper hardenability heat treatment to produce a hardened surface and a toughened core as the microhardness at the surface and the core were found to be in the range 254-294 HV. In addition, the metallography shows ferrite and pearlite microstructures at both the surface and the core of the failed axle. The SEM analysis of the fractured surface reveals the presence of burnished and crystalline surfaces. This shows that the failed axle does not meet the standard for the axle in terms of chemical, microstructure and hardness properties. The failure of the axle is typical of a fatigue failure.

Keywords: tricycle; surface; microhardness; microstructure; chemical composition

1. Introduction

Tricycles (**Figure 1**) have become a means of transportation in Africa and Asia such as Nigeria and India respectively. Some parts of the tricycle, especially the front axle wheel, are prone to failure. In a tricycle, an axle wheel is used to connect the wheels for the transmission of power and rotation. In service, axles are subjected to bending stresses which may cause possible misalignment between the axle and the bearing. As a result, axles are prone to fatigue and fatigue failures are of the rotating-bending and reversed (two-way) bending type (Asi, 2006).

Figure 1. Tricycle vehicle and position of front wheel axle

Several works have reported the failure analysis of axle parts of vehicles which may arise due to several reasons. For example, Huang and Zhu (2008) studied the failure analysis of friction weld in the truck axle and found that a significant amount of oxides and microporosity were found on the fractured part. Tawancy and Al-Hadhrami (2013) studied the failure of the rear axle of an automobile due to improper heat treatment. It was found that though the chemical composition of the axle was up to standard, however, microstructure and microhardness value of the axle were not up to standard due to improper heat treatment. In another research, Lemberg, Ellis and Guyer (2017) conducted research on a failure of the trunion axle on a hard suspension multi-axle trailer. Analysis reveals that a preexisting flaw in the axle was likely the driving force for the failure. In addition, Shad and ul Hasan (2018) studied the failure analysis of tractor axle wheels. It was found out that the induction-hardened axle was left without tempering and it appeared likely that quenching stresses in the induction-hardened layer of the axle which was left un-tempered were responsible for the cracking.

Hardenability heat treatment by flame hardening and induction hardening is used to heat treat the axle of vehicles to produce a hardened surface and toughened core to improve its mechanical properties. In addition, hardenability heat treatment is applied to plain carbon steels and low alloy steels containing 0.45-0.55% carbon (Rudnev, 2008). Flame hardening is a traditional method of case hardening of low and medium-carbon steels (Thamilarasan, Karunagaran and Nanthakumar, 2021). Flame hardening is a process in which the surface of a material is heated to recrystallization temperature and quenched in water (Jeyaraj *et al.*, 2015). Induction heating has gained prominence in producing case-hardened components such as axles with martensitic hardened surfaces and toughened cores. Induction heating technology is

nowadays the heating technology of choice in many industrial, domestic, and medical applications due to its advantages regarding efficiency, fast heating, safety, cleanness, and accurate control (Lucia *et al.*, 2014). However, improper hardenability heat treatment may result in catastrophic failure of case-hardened parts in service. Haghshenas and Savich (2019) reported that one of the key automobile engine components which almost always goes through some surface hardening is the transmission output axle and improper hardening of these components can create serious issues (i.e., catastrophic fracture) during actual service.

A lot of work has been carried out on failure analysis of vehicle axles; however, there is no report on the failure of a front wheel axle of a tricycle. The objective of this work is to investigate the failure of a tricycle axle using chemical composition, hardness, optical microscopy and SEM analyses.

2. Materials and Methods

The failed axle of a tricycle (**Figure 2**) was obtained from local repairers of tricycle vehicles and the elemental chemical composition was determined using SPECTROMAXX metal analyzer. The surface of the broken axle (surface and core) was ground with grit papers in the range of 80-1200 with the aid of water as a lubricant. The ground sample was polished on a polishing cloth using 1 μm alumina and the hardness from the surface to the core was recorded using microhardness with VTS Vickers Digital Micro Hardness Tester with a 1 kg hard steel testing load according to ASTM E384-17. (ASTM E384-17, 2017)

Figure 2. Fractured surface of a failed tricycle front wheel axle

The optical microscopy of the core and the surface was studied using an optical microscope. The samples were cut and mechanically ground on grades of silicon carbide grit papers in the range 240-1200 using water as the lubricant. Final polishing was achieved using 1 µm alumina powder suspended in distilled water. In addition, the polished samples were etched with nital etchant to reveal the microstructure and were recorded using an OMAX microscope. The micrographs were recorded using a metallurgical microscope OMAX microscope with an inbuilt camera. The SEM images of the fractured surface at the surface and the core were recorded using the JOEL-JSM 7600F machine. The schematic diagram of the axle of a tricycle is shown in

Figure 3.

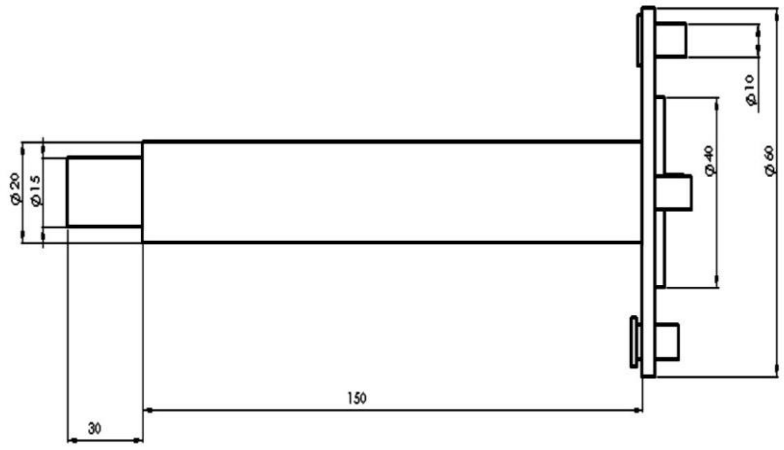

Figure 3. Schematic diagram of tricycle axle (all dimensions in mm)

3. Results and Discussion

3.1. Chemical Composition

The chemical composition of the failed front axle of a tricycle and the standard AISI 4140 composition of axles are shown in **Table 1**. From the table, it shows that the carbon content of the failed axle is 0.354%. This shows that the carbon content is below the standard for axles, which lies in the range of 0.38-0.43 (Tawancy and Al-Hadhrami, 2013). Carbon in steel plays a major role in improving the strength and hardness of steel by forming cementite with iron. In addition, carbon improves the hardenability of steels during hardenability heat treatment (Wei *et al.*, 2018). Carbon increases the hardenability of steels by allowing hard and brittle martensite to form during rapid cooling (quenching) and retards the formation of ferrite and pearlite. During hardenability, carbon atoms do not have time to diffuse out of the crystal in large amounts to form cementite (Allen and Boardman, 2005). In addition, beneficial elements

such as Mn, Cr, and Mo (with percentages 0.610%, 0.332% and 0.036% respectively), which improve hardness, strength, toughness and hardenability are below standard as reported in the literature (Wang *et al.*, 2021).

This shows that the steel used for the fabrication of the failed axle falls below the standard chemical composition requirement of steel for the fabrication of axles. For example, Mn allows an increase in hardness and strength at a slower quenching rate to reduce the defects forming during heating and quenching (Allen and Boardman, 2005). Likewise, Cr helps improve the strength, hardness and ability of the steel to be heat treated (Allen and Boardman, 2005). Lastly, Mo increases the hardenability during the heat treatment process by lowering the required quenching rate (Allen and Boardman, 2005). However, harmful elements P and S which cause cold and red shortness respectively were found to be low in the failed axle compared to those reported in the literature (Tawancy and Al-Hadhrami, 2013).

Table 1. Chemical composition of the front axle of a tricycle

Elements (%)	Failed axle	AISI 4140 Steel (Tawancy and Al-Hadhrami, 2013)
C	0.354	0.38-0.43
Si	0.191	0.15-0.35
Mn	0.610	0.71-1.00
P	0.0089	0.035
S	0.012	0.040
Cr	0.332	0.80-1.10
Mo	0.036	0.15-0.25
Fe	Balance	Balance

3.2. Microstructure at the Surface and the Core of Failed Axle

The microstructure of the failed axle obtained through metallography is shown in

Figure 4. The figure shows the presence of relative fine pearlite (dark phase) and fine ferrite (white phase) in the microstructure in

Figure 4(a). In contrast, steels that undergo hardenability heat treatment contain tempered martensite in their microstructure at the surface of the steels, which is in the form of needle shape/acicular structures as reported by Wei *et al.* (2018) and Tawancy and Al-Hadhrami (2013). This anomaly in the microstructure of the failed surface of the axle may be attributed to improper heat treatment or no heat treatment was conducted. The axle was supposed to be

heated above the A3 for low and medium-carbon steels on the iron-carbon equilibrium diagram to obtain a full austenite microstructure before quenching.

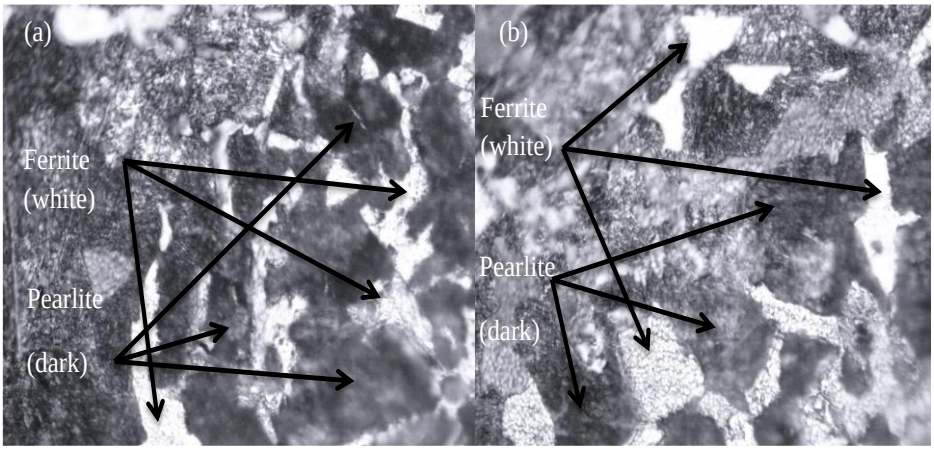

Figure 4. Optical microstructure of failed axle (a) at *the* surface and (b) at core 500X

The core of the failed axle (

Figure 4b), shows a similar microstructure to that at the surface (pearlite and ferrite), however, the phases are relatively coarser than that at the surface. This microstructure is expected at the core of an axle since axles are surface-hardened to give a hardened case and a toughened core. The pearlite and ferrite microstructures are responsible for the tougher core of the axle, as they are expected to absorb energy before fracture, which is in contrast to the martensitic case which is supposed to acquire high hardness and strength.

3.3. Hardness Profile of Failed Axle

The microhardness profile of the failed axle is shown in **Figure 5**. From the figure, it shows the hardness profile of the failed axle at the core and the surface does not conform to what is obtained from the literature on a hardenable axle. The hardness values at the surface range from 277-295 HV while at the core the hardness values range from 254-258 HV. This shows that the hardness values at the surface lie below the expected hardness of axles, which is in the range of 500-550 HV. Similarly, the hardness values at the core were below that reported by some literature (285 HV) (Asi, 2006; Tawancy and Al-Hadhrami, 2013). These low hardness values at the surface can be attributed to the presence of pearlite and ferrite at the surface of the failed axle instead of tempered martensite. This further confirms that the axle was given improper heat treatment or not quenched and tempered at all. At the core, the low value of the hardness can be attributed to the low carbon content of the axle (**Table 1**) which is below the standard of carbon content required for the axle. Literature has reported that carbon in steels

improves hardness, strength and hardenability by optimizing the variant selection to increase the density of high-angle grain boundary (Tawancy and Al-Hadhrami, 2013). In addition, other alloying elements such as Mn, Cr and Mo improve the strength, hardness, toughness and hardenability of low-carbon steels (Allen and Boardman, 2005).

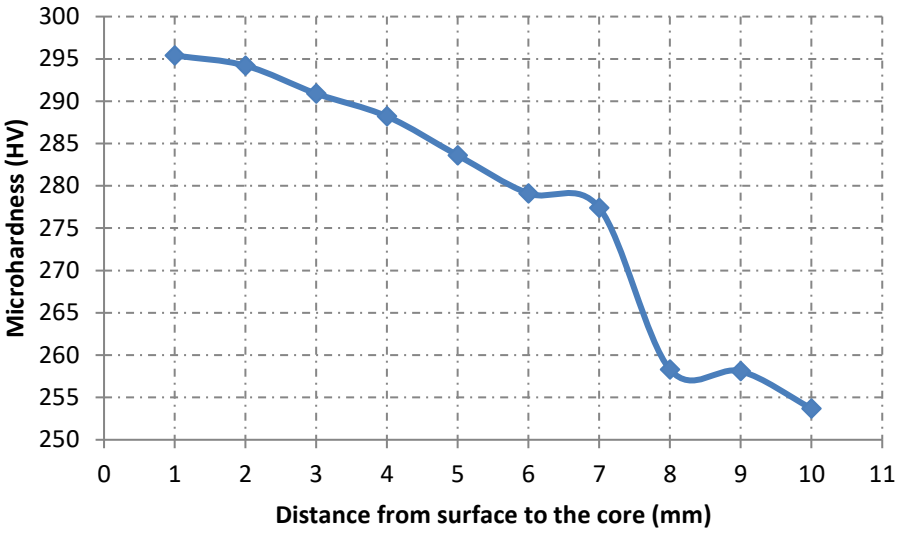

Figure 5. Hardness profile of failed tricycle axle

3.4. Macroscopic and SEM Analysis of the Failed Axle

The SEM analysis of the fractured surface is shown in **Figure 6**. From the figure, it shows two distinct regions of the failed axle-surface and the core. One is the burnished surface which shows that the parts have been rubbed before the final failure (**Figure 6a**). The other section of the failed part shows a crystalline failure, which shows the final failure of the parts. This type of failure is typical of fatigue. The burnished surface indicates that there was rubbing of the parts before the final failure. The core section (**Figure 6b**) shows a crystalline type of fracture, which shows that the toughened core has absorbed lower energy before the final fracture. In addition, this region represents a dimpled fracture, which is a characteristic failure of ductile materials (Al Jabbari *et al.*, 2018). This further confirms the presence of soft and ductile ferrite and pearlite at the core. In fatigue failure, cracks or flaws normally form at the surface of the piece which propagates and results in the final failure/fracture. In this type of axle where the hardness is not up to standard, the initiation of crack and its propagation will be easier.

In addition, **Figure 7** shows the macroscopic and SEM images of the fractured surface. The figure shows the presence of ratchet marks separating the different fatigue zones in several locations on the circumference of the failed axle (**Figure 7a**). These irregular fatigue-shaped

cracks initiated from the circumference of the axle and propagated towards the center. A similar observation was reported by Al Jabbari *et al.* (2018). **Figure 7(b)** shows the presence of craze lines, which is evidence of propagation of the crack front during fatigue failure. Craze lines are characterized by conical-shaped features in **Figure 7(b)**. The remainder of the crack propagation occurs through both the primary and secondary craze formation (Khan, Merah and Saghi, 2007). Ratchet marks are macroscopic and in contrast, craze lines are microscopic. The presence of ratchet marks and craze lines in the failed axle further proved that the failed axle is under cyclic stress (Jeyaraj *et al.*, 2015; Puliyaneth *et al.*, 2018; Yan *et al.*, 2018).

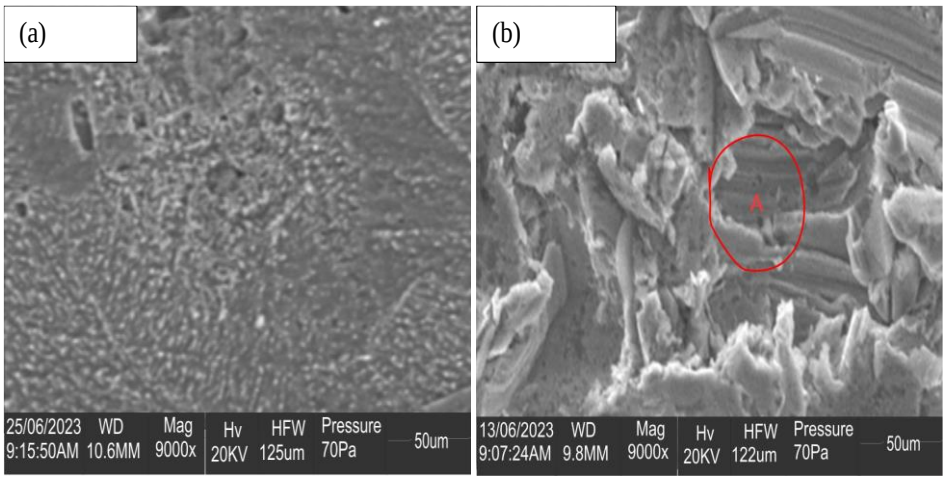

Figure 6. (a) SEM micrograph of the burnished surface of a failed wheel axle and (b) SEM micrograph of a crystalline core of a failed wheel axle

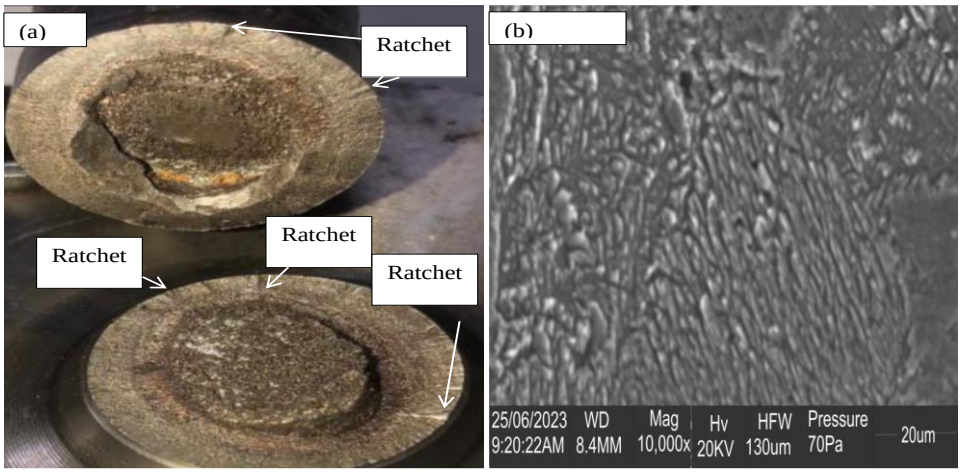

Figure 7. Macrograph and SEM micrograph of fractured axle (a) ratchets and (b) craze lines

To avoid failure of the front wheel axle of a tricycle, agencies saddled with the responsibility of ensuring quality control such as Standard Organization of Nigeria should be investigating the quality of axles in terms of chemical, mechanical and microstructural properties.

4. Limitation and Recommendation

This study does not take into consideration the improvement of chemical composition and case hardening of the front wheel axle. Therefore, further works should consider the improvement of chemical composition and case hardening of the spare parts of the front axle wheel to meet the standard.

5. Conclusion

This study was conducted on a failed front wheel axle of a tricycle. The chemical composition of the failed axle lies below that of the standard axle reported in the literature. In addition, the hardness of the failed axle at the surface and the core is below the values of hardness obtained for axles. The microstructure at the surface and the core shows the presence of pearlite and ferrite at both the surface and the core instead of tempered martensite at the surface and pearlite and ferrite at the core. Furthermore, the SEM analysis reveals that the failure of the axle is due to fatigue. From the results, it shows that the front wheel axle of tricycles in Nigeria does not meet the standard and this leads to the rampant failure of the axles.

Acknowledgement

Special thanks go to Department of Mechanical Engineering, Bayero University Kano, Nigeria for providing fund assistance and staff of Materials Science Laboratory of Bayero University Kano, Nigeria for conducting some of the test.

Credit Author Statement

Conceptualization, Abubakar M. and Tijjani Y.; Methodology, Saminu J.; Formal analysis, Kabir A, S.; Investigation, Eneojo E. U.; Resources, Kabir A. S. Isah J. and Eneojo E. U.; Data curation, Abubakar M; Writing—original draft preparation, Abubakar M.; Writing—review and editing, Tijjani Y.; Visualization, B.C.; Abubakar M., Tijjani Y. and Saminu J.; Project administration, Abubakar M.; Funding acquisition, Kabir A. S. Eneojo E. U. and Isah J.

Conflicts of Interest

The authors declare no conflict of interest.

References

Al Jabbari, Y.S. *et al.* (2018) 'Failure analysis of eleven Gates Glidden drills that fractured intraorally during post space preparation. A retrieval analysis study', *Biomedizinische Technik*, 63(4), pp. 407–412. Available at: https://doi.org/10.1515/bmt-2016-0245.

Allen, C.M. and Boardman, B. (2005) *ASM Handbook, Volume 1: Properties and Selection: Irons, Steels, and High-Performance Alloys*.

Asi, O. (2006) 'Fatigue failure of a rear axle shaft of an automobile', *Engineering Failure Analysis*, 13(8), pp. 1293–1302. Available at: https://doi.org/10.1016/J.ENGFAILANAL.2005.10.006.

ASTM E384-17. (2017) Standard Test Method for Microindentation Hardness of Materials.

Haghshenas, M. and Savich, W. (2019) 'Fixing Induction Heat Treatment Flaws of an Automotive Transmission Output Shaft', *Journal of Failure Analysis and Prevention*, 19(1), pp. 106–114. Available at: https://doi.org/10.1007/s11668-018-0572-8.

Huang, Y. and Zhu, Y. (2008) 'Failure analysis of friction weld (FRW) in truck axle application', *Journal of Failure Analysis and Prevention*, pp. 37–40. Available at: https://doi.org/10.1007/s11668-007-9097-2.

Jeyaraj, S. *et al.* (2015) 'Optimization of Flame Hardening Process Parameters Using L9 Orthogonal Array of Taguchi Approach', *International Journal of Engineering and Applied Sciences (IJEAS)*, 2(3), pp. 40–44. Available at: www.ijeas.org.

Khan, Z., Merah, N. and Saghi, F. (2007) 'Fatigue crack growth process in CPVC pipe couplings', *E-Polymers* [Preprint]. Available at: https://doi.org/10.1515/epoly.2007.7.1.703.

Lemberg, J.A., Ellis, B.D. and Guyer, E.P. (2017) 'Failure of a Trunnion Axle on a Hard Suspension Multi-axle Trailer', *Journal of Failure Analysis and Prevention*, 17(2), pp. 189–194. Available at: https://doi.org/10.1007/s11668-017-0236-0.

Lucia, O. *et al.* (2014) 'Induction heating technology and its applications: Past developments, current technology, and future challenges', *IEEE Transactions on Industrial Electronics*, 61(5), pp. 2509–2520. Available at: https://doi.org/10.1109/TIE.2013.2281162.

Pantazopoulos, G., & Vazdirvanidis, A. (2008). Fractographic and metallographic study of spalling failure of steel straightener rolls. Journal of Failure Analysis and Prevention, 8(6), 509–514. https://doi.org/10.1007/s11668-008-9170-5

Puliyaneth, M. *et al.* (2018) 'Study of ratchet limit and cyclic response of welded pipe', *International Journal of Pressure Vessels and Piping*, 168, pp. 49–58. Available at: https://doi.org/10.1016/J.IJPVP.2018.09.004.

Rudnev, V. (2008) 'Induction Hardening of Gears and Critical Components', *Gear Technology*, pp. 58–63.

Shad, M.R. and ul Hasan, F. (2018) 'Failure Analysis of Tractor Wheel Axle', *Journal of Failure Analysis and Prevention*, 18(6), pp. 1631–1634. Available at: https://doi.org/10.1007/s11668-018-0561-y.

Tawancy, H.M. and Al-Hadhrami, L.M. (2013) 'Failure of a rear axle shaft of an automobile due to improper heat treatment', *Journal of Failure Analysis and Prevention*, pp. 353–358. Available at: https://doi.org/10.1007/s11668-013-9682-5.

Thamilarasan, J., Karunagaran, N. and Nanthakumar, P. (2021) 'Optimization of oxy-acetylene flame hardening parameters to analysis the surface structure of low carbon steel', *Materials Today: Proceedings*, 46, pp. 4169–4173. Available at: https://doi.org/10.1016/J.MATPR.2021.02.680.

Wang, C. *et al.* (2021) 'Microstructure and mechanical properties of a novel medium Mn steel with Cr and Mo microalloying', *Materials Science and Engineering: A*, 825, p. 141926. Available at: https://doi.org/10.1016/J.MSEA.2021.141926.

Wei, J. *et al.* (2018) 'Influence of heat treatments on microstructure and mechanical properties of Ti-26Nb alloy elaborated in situ by laser additive manufacturing with Ti and Nb mixed powder', *Materials*, 12(1). Available at: https://doi.org/10.3390/ma12010061.

Yan, Z. *et al.* (2018) 'Deformation behaviors and cyclic strength assessment of AZ31B magnesium alloy based on steady ratcheting effect', *Materials Science and Engineering: A*, 723, pp. 212–220. Available at: https://doi.org/10.1016/J.MSEA.2018.03.023.